Hyperpolarized ^{129}Xe Nuclear Magnetic Resonance Studies of Isoreticular Metal-Organic Frameworks

Shane Pawsey,* Igor Moudrakovski, and John Ripmeester

Steacie Institute for Molecular Sciences, Ottawa, Ontario, Canada K1A 0R6

Li-Qiong Wang* and Gregory J. Exarhos

Fundamental Science Division, Pacific Northwest National Laboratory, Richland, Washington 99354

Jesse L. C. Rowsell and Omar M. Yaghi†

Department of Chemistry, University of Michigan, 930 North University Avenue, Ann Arbour, Michigan 48109

Received: October 17, 2006; In Final Form: January 22, 2007

The pore environments of a series of isoreticular metal-organic frameworks (IRMOF) have been studied using hyperpolarized (HP) ^{129}Xe nuclear magnetic resonance (NMR) spectroscopy. Xenon gas behaved as an efficient probe molecule for interrogating the variability of adsorption sites in functionalized IRMOF materials through variations in the NMR chemical shift of the adsorbed xenon. The xenon adsorption enthalpies extracted from variable-temperature HP ^{129}Xe NMR were found to be lower than published values for the physisorption of xenon. The low heats of adsorption were corroborated by xenon adsorption measurements that revealed two atoms per pore under one atmosphere of pressure at 19 °C. Average pore diameters estimated from the empirical chemical shift and pore size correlations based on a geometrical model were compared with X-ray crystallography data. The exchange processes of xenon in IRMOFs also were explored using 2D exchange spectroscopy (EXSY) ^{129}Xe NMR. It was found the exchange of xenon from adsorption sites within the IRMOF to the free gas space is much slower than that between the adsorption sites within the lattice. Cross-polarization experiments showed that the preferred adsorption sites were spatially removed from the phenylene rings of the network. This agrees with previous spectroscopic, structural, and computational studies of gas adsorption (H_2, N_2, Ar) in IRMOFs that indicate the preferred binding sites reside near the carboxylate groups of the inorganic clusters.

Introduction

Isoreticular metal organic frameworks (IRMOFs) first synthesized by Eddaoudi and co-workers[1,2] are stable, crystalline, porous materials with cubic topologies and exceptionally high surface areas. Their large adsorption capacities for gases such as H_2, CH_4, and CO_2 have led to significant interest in applications such as catalysis, molecular separation, and gas storage.[3,4]

The ability to functionalize the organic linking groups of these materials allows for tailoring of the dimensions and chemical environments of the pores. IRMOFs are prepared by a self-assembly process. The basic structure consists of oxide-centered Zn_4O clusters bridged by carboxylate-functionalized molecules resulting in an extended three-dimensional, highly porous cubic network (Figure 1). Through the use of different linking groups, frameworks containing various chemical functionalities and pore sizes have been prepared. The original linking group used to synthesize these materials was benzene-1,4-dicarboxylate (BDC), which produced the prototype structure MOF-5 (=IRMOF-1).[2] To modify the pore environment, functional groups were added to the phenylene ring: IRMOF-2 has been brominated at position 2, IRMOF-3 is functionalized with an amino group at the same position, and IRMOF-6 has an ethylene group linking positions 2 and 3.

The rational design of next-generation gas storage materials requires a detailed understanding of the IRMOF pore environments. The adsorption sites and structure of the resident pores can be characterized by powerful spectroscopic techniques such as inelastic neutron scattering[5,6] and infrared spectroscopy[7] of adsorbed H_2 and nuclear magnetic resonance spectroscopy of ^{129}Xe. To date, hyperpolarized (HP) ^{129}Xe NMR has been used to study porous systems like zeolites,[8,9] aluminophosphates,[10−12] polymers,[13−16] and organic zeolite isomorphs.[17] Unlike the previously studied materials, the IRMOFs are novel open-pore materials with significantly higher surface areas. This paper presents the first study of this type of novel open-pore materials using HP ^{129}Xe NMR.

Over the years, ^{129}Xe NMR has developed into a powerful and robust method for studying porous solids.[18−21] The large chemical shift range of ^{129}Xe is strongly dependent on environmental and chemical factors such as the composition of the adsorbent and nature and concentration of coadsorbed molecules and the shape and size of resident void spaces. As compared with X-ray powder diffraction measurements, transmission electron microscopy, and gas adsorption isotherm measurements, which in principle provide information on pore size, pore volume, and surface area, ^{129}Xe NMR spectroscopy has the

* To whom correspondence should be addressed. E-mail: lq.wang@pnl.gov (L.-Q. W.); shane.pawsey@nrc-cnrc.gc.ca (S. P.).

† Current address: Department of Chemistry and Biochemistry, University of California, Los Angeles, CA 90095.

10.1021/jp0668246 CCC: $37.00
Published on Web 04/03/2007

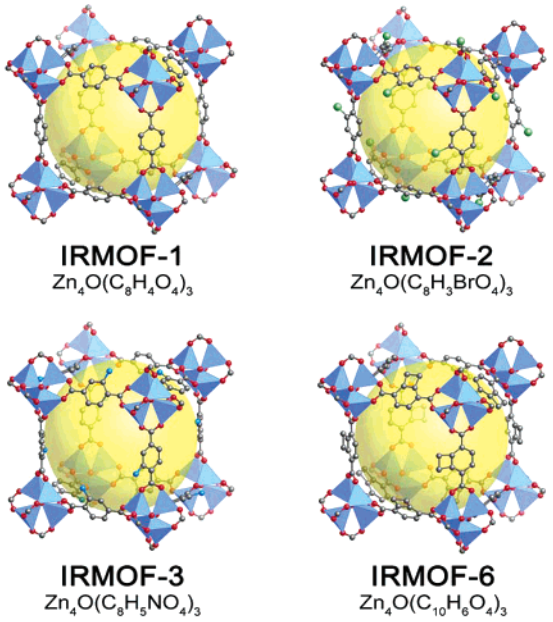

Figure 1. Portions of the crystal structures of IRMOF-1, IRMOF-2, IRMOF-3, and IRMOF-6 highlight the relatively large pores available for gas adsorption (shown as yellow spheres). Only one orientation of the disordered linking moieties is shown in each case. Atom colors: Zn blue tetrahedra, O red spheres, C black spheres, Br green spheres, N blue spheres, H not shown.

advantage of probing the connectivity and the uniformity of the pores not accessible by other techniques. The use of optical pumping techniques for the production of hyperpolarized xenon allows a dramatic increase in the sensitivity of ^{129}Xe NMR to a factor of 10^4.[22] With HP xenon produced under continuous flow (CF) conditions, measurements are possible at very low concentrations of xenon, which makes the contribution to the chemical shift of Xe−Xe interactions on the surface very small. The observed ^{129}Xe chemical shifts can be assigned principally to the interactions between the xenon atoms and the surface of the porous materials. Hence, the technique can successfully probe the pore structure and connectivity. Temperature-dependent chemical shift spectra and 2D exchange spectroscopy (EXSY) CF ^{129}Xe NMR were used to obtain a better understanding of the pore structure, the uniformity of the adsorption sites, and the pore network interconnectivity.

Experimental Section

Materials. The IRMOF materials used in this work were prepared by procedures previously described.[1,23] To minimize exposure of IRMOFs to atmospheric moisture, samples were stored and handled in a glove box under an inert argon atmosphere. Samples of IRMOFs for continuous flow HP ^{129}Xe NMR were packed in standard 7.5 mm Chemagnetics rotors. Sealed samples to be studied by thermally polarized ^{129}Xe NMR were prepared by evacuating the materials in a 5 mm OD glass tube on a vacuum line (10^{-6} Pa) at room temperature for several hours followed by freezing known amounts of Xe with liquid N_2 and flame sealing.

Adsorption Measurements. Xe adsorption isotherms were obtained at room temperature on a home-built adsorption apparatus using a standard volumetric technique with a range of Xe pressure between 10 and 1000 KPa.[24] Samples were outgassed for 12 h at 100 °C under vacuum (10^{-6} Pa) prior to measurements.

^{129}Xe NMR Measurements. ^{129}Xe NMR measurements were performed on a Bruker Avance-200 instrument operating at 55.3 MHz (magnetic field of 4.7 T) using a continuous flow of HP Xe. A Chemagnetics 7.5 mm Pencil probe modified for CF, similar to that previously reported,[25] was employed for HP flow experiments. The continuous flow polarizer for the production of HP Xe was of a design similar to that previously reported.[26,27] A 80 W CW diode laser from Coherent operating at a wavelength of 785 nm was used as the excitation source. A xenon−helium−nitrogen mixture with a volume composition of 1%−96%−3% was used in all CF HP experiments. The flow rate was monitored with a Vacuum General flow controller (Model 80-4) and was kept constant in the range of 200−250 scc/min (gas flow normalized to standard conditions). In the CF HP experiments, a flow of HP xenon was delivered directly into the coil region of the NMR probe through 1.5 mm ID plastic tubing excluding air from entering the system. Variable-temperature NMR experiments in the 170−400 K range were performed using a Varian VL950 temperature controller. The temperature inside the NMR coil of the CF probe was calibrated using the ^{207}Pb resonance in $Pb(NO_3)_2$.[28] 2D-EXSY spectra were obtained using the standard sequence described elsewhere.[29−34] The 2D-EXSY and cross-polarization (CP) experiments were performed on a Bruker AMX-300 spectrometer with a Morris Instruments Inc. probe. IRMOF samples were sealed under 1−2 atm of xenon gas. The reported ^{129}Xe NMR chemical shifts were referenced to xenon gas extrapolated to zero pressure.

Results and Discussion

Hyperpolarized ^{129}Xe NMR Spectra. ^{129}Xe NMR of IRMOFs using continuous flow polarization is performed at very low partial pressures of xenon. Under these conditions, the spectra correspond to very low Xe loadings with minimal Xe−Xe interactions contributing to the chemical shift. Temperature-dependent HP ^{129}Xe NMR spectra for IRMOF-1, IRMOF-2, IRMOF-3, and IRMOF-6 are shown in Figure 2. Despite the similar frameworks and pore sizes reported for these materials, spectra collected for each of the four samples exhibited different line shapes and temperature dependencies. These differences suggest that the functional groups on the organic linkers affect the adsorption sites occupied by xenon atoms. For the purposes of the xenon NMR experiments, an adsorption site has been defined as the localized area or region sampled by xenon atoms during the acquisition time. The chemical shifts of ^{129}Xe NMR signals are averaged when rapid exchange exists between the adsorption sites being probed. Averaging can also occur between the adsorption sites and the free-gas-phase Xe when exchange is sufficiently rapid. Therefore, it is likely that for some systems one cannot assign a particular chemical shift to a specific adsorption site or structural feature at a given temperature because of the rapid exchange processes. As shown in Figure 2a, the HP ^{129}Xe spectrum of IRMOF-1 at room temperature displays a prominent peak for adsorbed xenon near 50 ppm with a broad shoulder in the vicinity of 60 ppm. The much less intense signal at 0 ppm corresponds to free xenon gas in the intercrystalline space. Upon cooling, the peak near 50 ppm and the accompanying shoulder (both assigned to adsorbed xenon) shift slightly downfield and become partially resolved. The less intense shoulder clearly represents an alternative environment, such as a smaller pore or site that restricts exchange with the environment associated with the more intense peak.

In contrast, the room-temperature HP ^{129}Xe spectrum of IRMOF-2 (Figure 2b) shows two intense, partially resolved signals at 62 and 70 ppm along with the weak free gas peak at 0 ppm. When the sample is cooled to −100 °C, the adsorbate chemical shifts increase and become completely resolved,

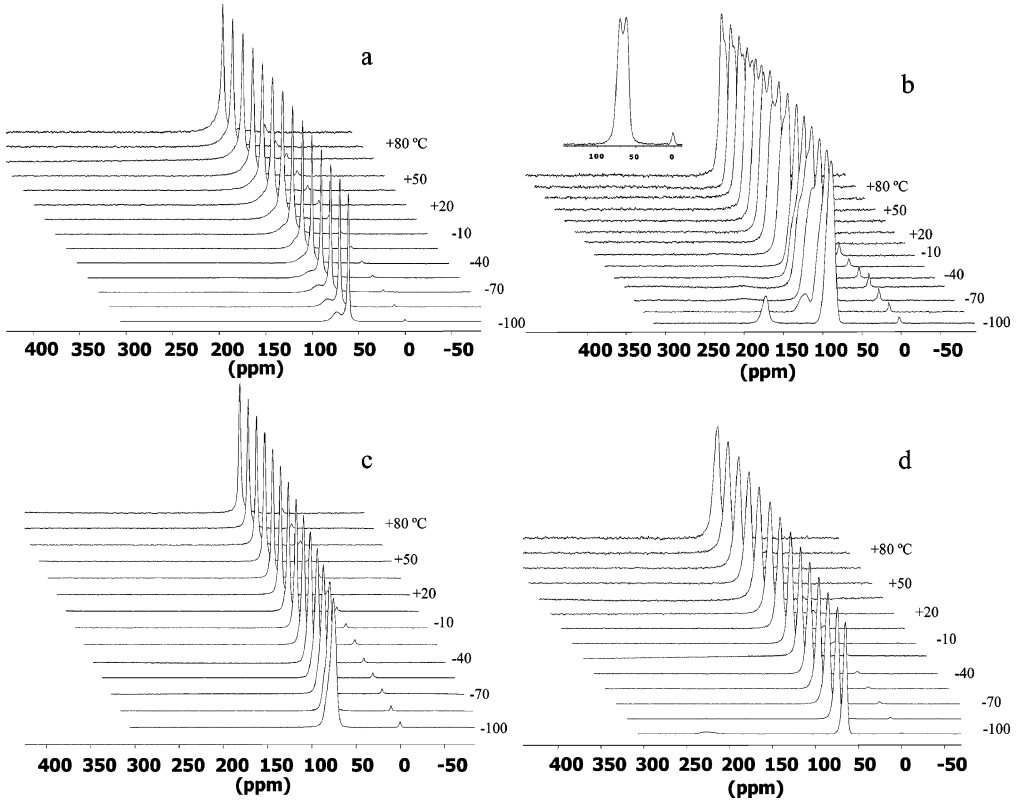

Figure 2. Variable-temperature CF HP ^{129}Xe NMR spectra for IRMOF-1 (a), IRMOF-2 (b), IRMOF-3 (c), and IRMOF-6 (d). Spectra were acquired at 15 °C intervals but only every other spectrum has been labeled for clarity. The inset in b is the 20 °C spectrum of IRMOF-2.

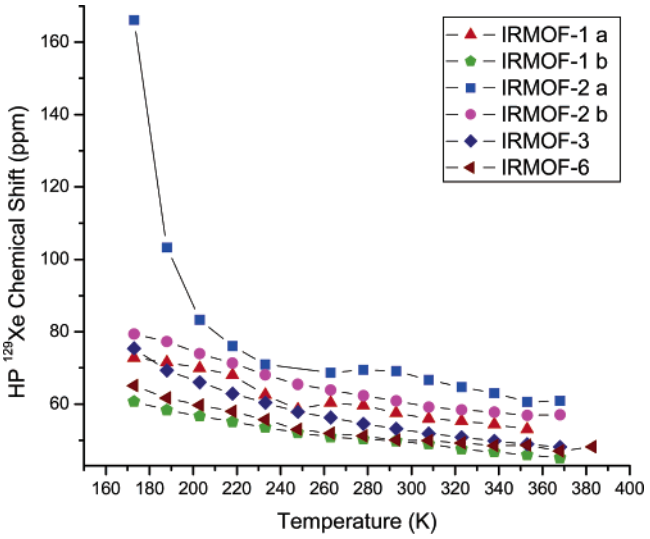

Figure 3. The ^{129}Xe chemical shift plotted as a function of temperature for IRMOFs. The "a" peaks represent the larger chemical shift signals and the "b" peaks are the lower chemical shift signals.

centered at 85 and 165 ppm. The larger chemical shift change of the downfield peak at the lowest temperatures may imply the presence of a new adsorption site. This new adsorption site is likely to have a slightly longer retention time for xenon at low temperature and therefore slower exchange between the adsorption sites. The slower exchange prevents the xenon molecules from sampling all available void space during the NMR acquisition time and results in separate peaks with shifts not averaged over all possible adsorption sites. The peak with the larger chemical shift is indicative of xenon within a smaller pore as compared to the other peak with the smaller shift. Upon heating, the less intense downfield peak shifts much closer to

TABLE 1: The Heats of Adsorption for Xenon with the IRMOF Samples along with the Estimated Pore Diameters on the Basis of Spherical (D_{sp}) and Cylindrical (D_c) Models Compared with the Fixed and Free Diameters Measured from the Reported Crystal Structures in Ref 1

sample	ΔH_{abs} (kJ/ mol)	D_{sp} (Å)	fixed (Å)	D_c (Å)	free (Å)
IRMOF-1(a)[a]	5.6	17.7	15.0	11.1	7.8
IRMOF-1(b)[a]	5.4	20.6		12.5	
IRMOF-2(a)[a]	5.0	16.7	12.8	10.5	5.5
IRMOF-2(b)[a]	17.3	15.0		9.7	
IRMOF-3	5.0	19.2	15.0	11.8	6.9
IRMOF-6	4.0	20.1	15.0	12.2	6.6

[a] (a) higher chemical shift peak, (b) lower chemical shift peak.

the other signal as shown in Figure 2b. Additionally, as the temperature is increased, the peak height of the higher shift resonance increased and at 20 °C becomes greater than the other signal. The sharpening of the peak indicates that the environment in which the xenon is located has become more homogeneous likely involving increased dynamic processes.

The HP ^{129}Xe NMR spectrum of IRMOF-3 (Figure 2c) at room temperature displays a strong and sharp peak at 55 ppm from xenon adsorbed in relatively large pores. Over a temperature range of −100 °C to +95 °C, the chemical shift of the adsorbed xenon is observed to move from approximately 75 to 48 ppm. The single resonance observed indicates an averaging of the chemical shifts from all sorption environments sampled by the xenon probe molecule because of unrestricted exchange.

The spectra collected from Xe in IRMOF-6 (Figure 2d) are similar to those for IRMOF-3 in that only a single peak is observed for adsorbed xenon and its chemical shift varies over a comparable range. However, variations in the peak shape as a function of temperature are noticeably different for these two materials. The resonance for adsorbed xenon in IRMOF-3

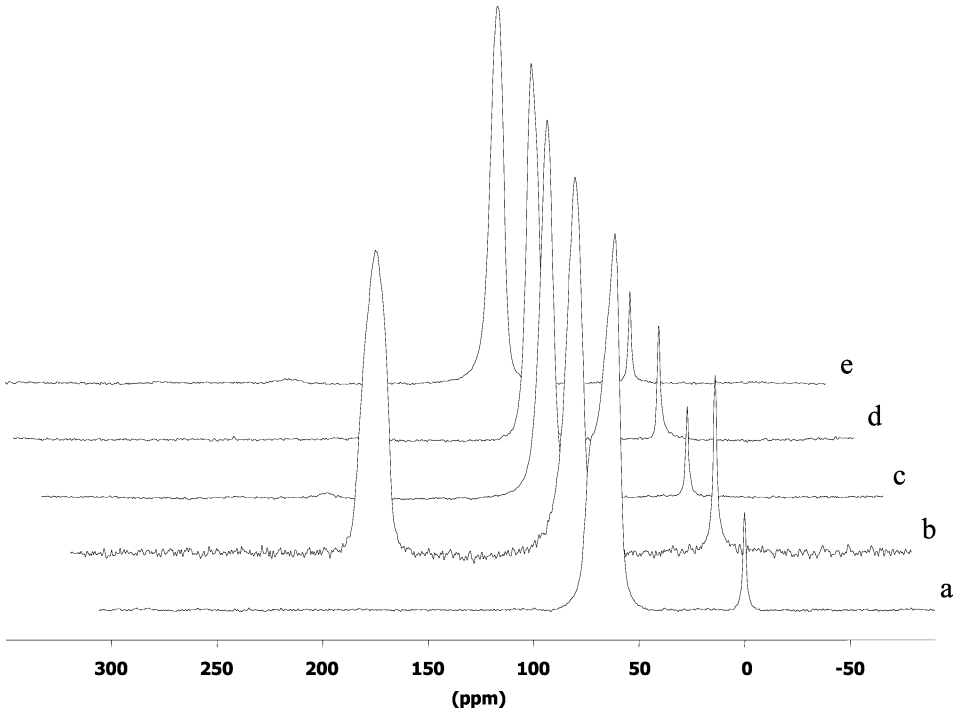

Figure 4. HP ^{129}Xe NMR spectra of IRMOF-2: (a) IRMOF-2, (b) methane added to flow, (c) sample under vacuum overnight after exposure to methane, (d) heated to 75 °C, and (e) returned to room temperature.

narrows with increasing temperature, while the opposite trend is observed for IRMOF-6. The peak narrowing with increasing temperature observed for IRMOF-3 is interpreted as resulting from an increased homogeneity of void space sampled by xenon, whereas in the case of IRMOF-6, it appears the environment sampled by xenon becomes less homogeneous as the temperature increases. The spectrum for IRMOF-6 at −100 °C displays a broad peak near 230 ppm that was not observed at higher temperatures. This chemical shift region is generally associated either with xenon adsorbed in tight sites or condensed liquid xenon. All of the above suggest that IRMOF-3 and IRMOF-6 have different pore environments and adsorption dynamics.

The multiple peaks observed in the ^{129}Xe NMR spectra reflect the heterogeneous surface structure of IRMOFs. The variation in chemical shifts and temperature-dependent line shapes in ^{129}Xe NMR spectra for IRMOF samples with different functional groups suggests that different sorption environment exists in each material. In addition to altering the geometry and polarizability of the local surface structure, the pendent functional groups will inductively affect the polarizability of the phenylene links to which they are bonded. This will alter the van der Waals interactions an adsorbate molecule encounters at specific adsorption sites, such as those previously identified by experimental[5−7,35−37] and computational[38−43] studies.

In the case of IRMOF-1, eight symmetry-independent sites were determined for the adsorption of argon from crystallography; several of these sites can also be populated by N_2 and H_2.[35−37] If xenon exchange is sufficiently slow between these adsorption sites, this could lead to the appearance of additional features in the ^{129}Xe spectra, however, this would depend on the barrier heights to exchange between the different sites. Although Xe is larger than H_2, N_2, and Ar, there is adequate void space within the IRMOF pores to accommodate several Xe atoms. In these experiments, a very low loading of Xe gas (1% of total gas flow) was used to reduce Xe−Xe interactions, however, Xe hopping between inequivalent sites will still give an exchange-averaged line shape. The two

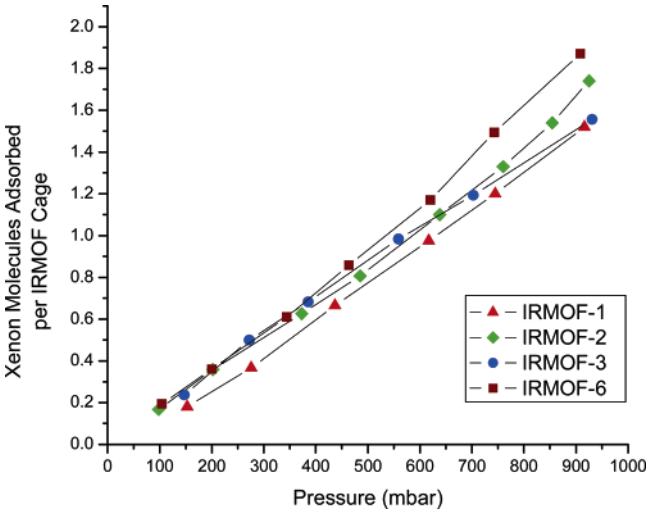

Figure 5. Xe adsorption isotherms for IRMOFs measured at 292 K.

adsorption peaks recorded in the HP ^{129}Xe spectra indicate that the diffusion barrier for those particular sites (or sets of sites) is large.

The spectra reflect an average of the fractional occupancies at the different adsorption sites of adsorbed Xe over the course of the NMR acquisition. In the case of IRMOF-2, the steric effect of the Br groups magnifies a common structural feature of the IRMOFs where half of the pores have the phenylene faces directed inward, while the phenylene edges point inward on the other half. This leads to a bimodal pore size distribution, and in the case of IRMOF-2 at low temperatures, it appears possible Xe is primarily adsorbed in one of the environments. As the temperature is raised, Xe begins to sample both environments. The small difference in chemical shift between the signals from adsorbed xenon indicates either rapid exchange or similarly sized pores.

Heats of Adsorption and Pore Sizes. The temperature dependence of the adsorbed ^{129}Xe chemical shifts is shown in

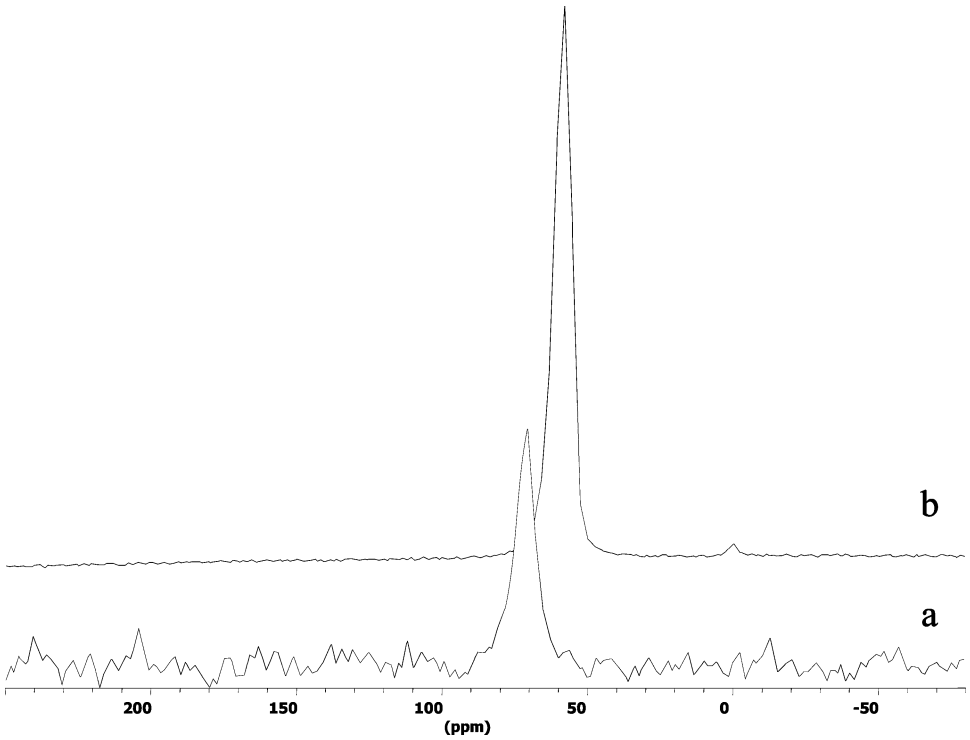

Figure 6. CP (a) and CF HP ^{129}Xe spectrum (b) for IRMOF-6 at −50 °C.

Figure 3. Fitting the data for these materials allows the xenon enthalpy of adsorption to be estimated. The procedure for the data analysis has been described in a previous publication.[44] With one exception, the ΔH_{abs} values for the IRMOF samples are between 4 and 8.4 kJ/mol (Table 1). These enthalpy of adsorption values for xenon are significantly lower than were reported for physisorbed xenon in organic aerogels,[45] porous silica,[44,46,47] and silylated mesoporous MCM-41.[48] The open structures of the IRMOF materials, which suggest weaker interactions with xenon when compared to the organic systems,[45] may be the reason for this difference in adsorption enthalpy. Tight sorption sites for xenon tend to be those where xenon is in contact with a maximum amount of surface (i.e., those with large chemical shifts such as the side pocket in mordenites), whereas "flat" surfaces give minimal opportunities for interaction. However, the enthalpy values compare favorably with those reported for H_2 adsorption.[7,39] Although determined by different methods, the ΔH_{abs} values determined here are about half of those reported for the adsorption of methane molecules, more of a similar size to xenon.[41]

The ΔH value that falls outside the above-mentioned range is associated with the higher chemical shift peak in the ^{129}Xe spectrum of IRMOF-2. The calculated value of 17.3 kJ/mol is in better agreement with typical values for physisorbed xenon.[44−48] This probably corresponds to the adsorption of xenon in a unique environment provided by the Br functionalized IRMOF or a region inaccessible in the other samples.

Using empirical chemical shift−pore size correlations developed to fit inorganic systems like MCMs and zeolites,[44,49] pore diameter estimates of the IRMOFs were attempted using a geometrical model. The results derived in the context of spherical and cylindrical models reported in Table 1 are to be treated as approximations. The pore sizes should be regarded with caution, as there may be an unaccounted scaling factor because of differences in the chemical composition. Considering the wide channels throughout the frameworks, the cylindrical pore model seems the most reasonable to describe these materials. The estimated values span a range from 9.7 to 12.5 Å. IRMOF-2 with two peaks for adsorbed xenon in the ^{129}Xe spectrum yields estimated room-temperature pore diameters of 9.7 and 10.5 Å for the high and low chemical shift peaks, respectively. The values estimated here result from an averaging of the bimodal pore distribution and are found to be larger than the reported values in the literature.[1]

In the case of IRMOF-1, the pore sizes estimated from the chemical shifts of the downfield shoulder and main peak, 11.1 and 12.5 Å, are notably larger than the free diameter of 7.8 Å determined crystallographically.[1] IRMOF-3 and IRMOF-6 with single signals for adsorbed xenon in the NMR spectra had cylindrical pore diameters of 11.8 and 12.2 Å, respectively. These values are almost twice as large as the 6.9 and 6.6 Å measured for IRMOF-3 and IRMOF-6, taking into account the van der Waals radii of the framework atoms. The discrepancies may be due to the differences in the chemical composition and morphology of the surfaces of the IRMOFs compared to the silicate materials from which the chemical shift−pore size correlations are derived. However, it is not unexpected that two such different techniques would yield such dissimilar results.[50] Xenon atoms will have experienced a variety of different environments as they pass through the IRMOF network with the phenylene rings and functional groups assuming different orientations because of their crystallographic disorder. These factors are not accounted for in the geometrical model used to calculate the pore size and could explain the discrepancies when compared to the previously reported values.

Competitive Adsorption of Xenon and Methane. HP ^{129}Xe experiments were modified by adding a stream of methane to the flowing gas mixture to probe for competitive sorption of the similarly sized xenon and methane molecules. Analogous experiments have been performed to investigate preferential adsorption phenomena.[51] There appears to be no effect on the ^{129}Xe spectrum upon the addition of methane in the cases of IRMOF-1, -3, and -6, aside from a decrease in the ^{129}Xe signal intensity because of dilution. IRMOF-2, however, displayed interesting results when methane was added to the flow. As shown in Figure 4, the addition of methane resulted

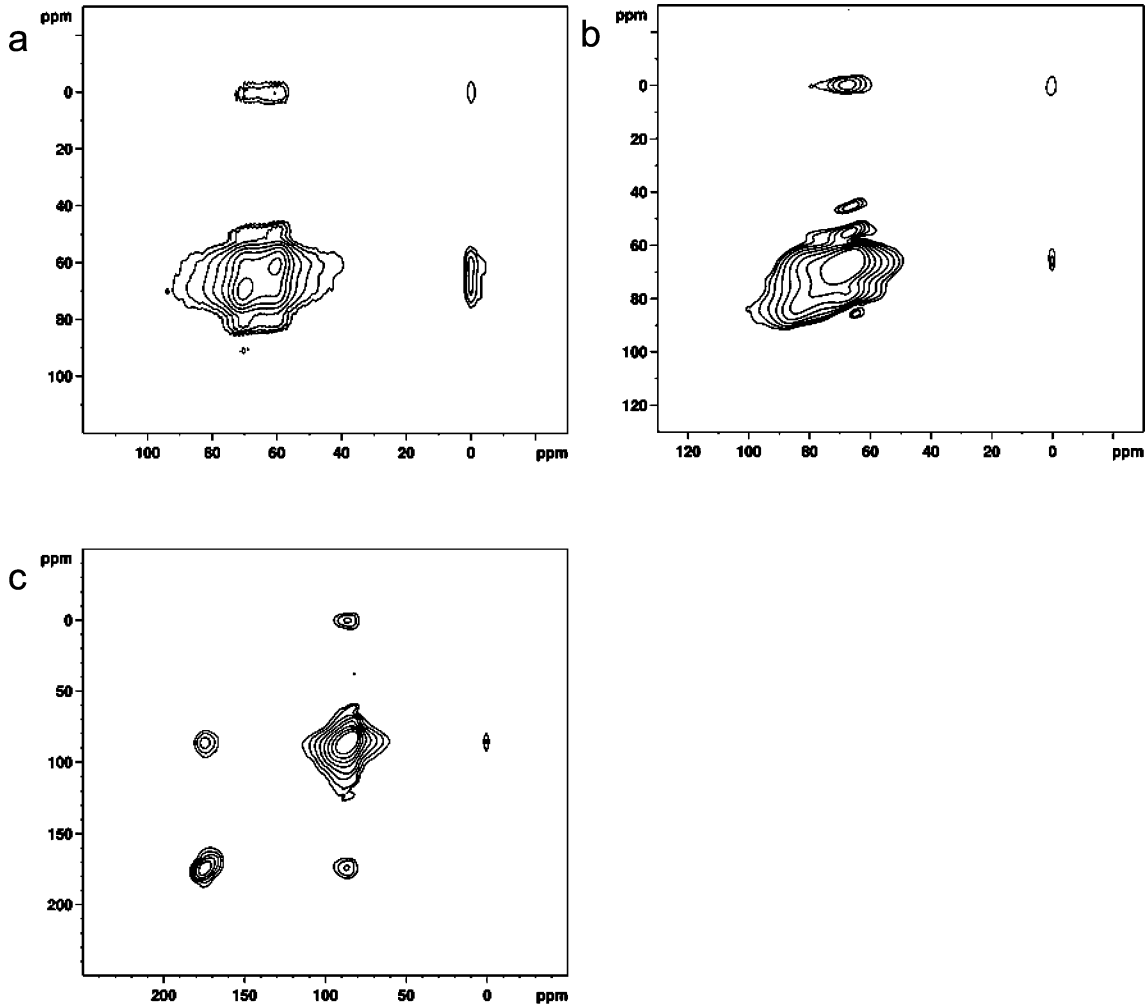

Figure 7. ^{129}Xe 2D EXSY NMR spectra of IRMOF-2 with 32 scans, 1 s repeat time, TD1 of 128 and a mix time of 50 ms at (a) 35, (b) −30, and (c) −100 °C.

in an adsorbed xenon signal around 170 ppm while the signal at 70 ppm dropped in intensity. After sufficient time, the peak near 170 ppm grew in intensity, while the peak at 70 ppm disappeared, leaving only the original signal at 62 ppm. After the methane flow was stopped, the signal near 170 ppm receded into the baseline; however, the peak at 70 ppm did not return. Even after heating the sample and leaving it under vacuum, the peak at 70 ppm did not return. The addition of methane to the gas stream appears to have an irreversible effect upon IRMOF-2 that either changes the structure of the framework or renders an adsorption site inaccessible to xenon molecules. The peak at 170 ppm may have resulted from the presence of multiple methane molecules along with the xenon atom within a cavity. This would cause the size of the void space to appear smaller from the perspective of the xenon molecule and result in the larger observed chemical shift. When the methane flow is stopped, the adsorbate signal is narrower giving an indication that IRMOF-2 is more crystalline after exposure to the methane flow which may have driven off residual impurities.

Xe Adsorption Isotherms. Xenon adsorption isotherms were measured to determine the amount of xenon actually residing in each IRMOF pore under the experimental conditions. Data was collected at 19 °C and pressures ranged from roughly 100 to 1000 mbar. The adsorption curves shown in Figure 5 are similar and have nearly linear pressure dependence without any tendency to approach saturation, thus showing Henry's law behavior. Over the initial part of the isotherm, all four IRMOF samples were found to contain roughly two xenon atoms per pore at 1 atm. Considering such small xenon occupancy, it is not surprising that only a single environment was observed for adsorbed xenon in some of the NMR data. With the low adsorption enthalpy values, xenon gas will exchange rapidly within the network thereby averaging the observed chemical shift.

Cross-Polarization and 2D EXSY Experiments. To better understand the location of xenon atoms within the IRMOF lattice and the exchange between different adsorption sites, ^{1}H−^{129}Xe cross-polarization[52,53] (CP) and two-dimensional exchange[54−57] (2D EXSY) experiments were performed on IRMOF samples sealed under 1−2 atm of xenon gas. Representative CP and CF HP ^{129}Xe NMR spectra for IRMOF-6 taken at −50 °C are shown in Figure 6. In general, for CP experiments to be successful, strong heteronuclear dipolar interactions must exist. Hence, the ^{129}Xe nuclei must be sufficiently close to ^{1}H nuclei as dipolar interactions have a $1/r^3$ dependence. Along with internuclear distance, molecular mobility also influences CP experiments. Overall, CP is a useful tool in establishing the proximity of coupled nuclei and following molecular dynamics in the solid state.[58] The only ^{1}H nuclei found in the IRMOF samples are on the phenylene rings or their pendent groups, and the xenon will need to be relatively close to the rings or pendent groups if it is to be observed. In the case of IRMOF-6, which has the most ^{1}H nuclei, a ^{129}Xe signal was observed at 70 ppm after 1024 scans with a 3 s pulse delay and an extended contact time of 15 ms when the temperature was dropped to −50 °C (Figure 6a). As compared with the CF HP ^{129}Xe

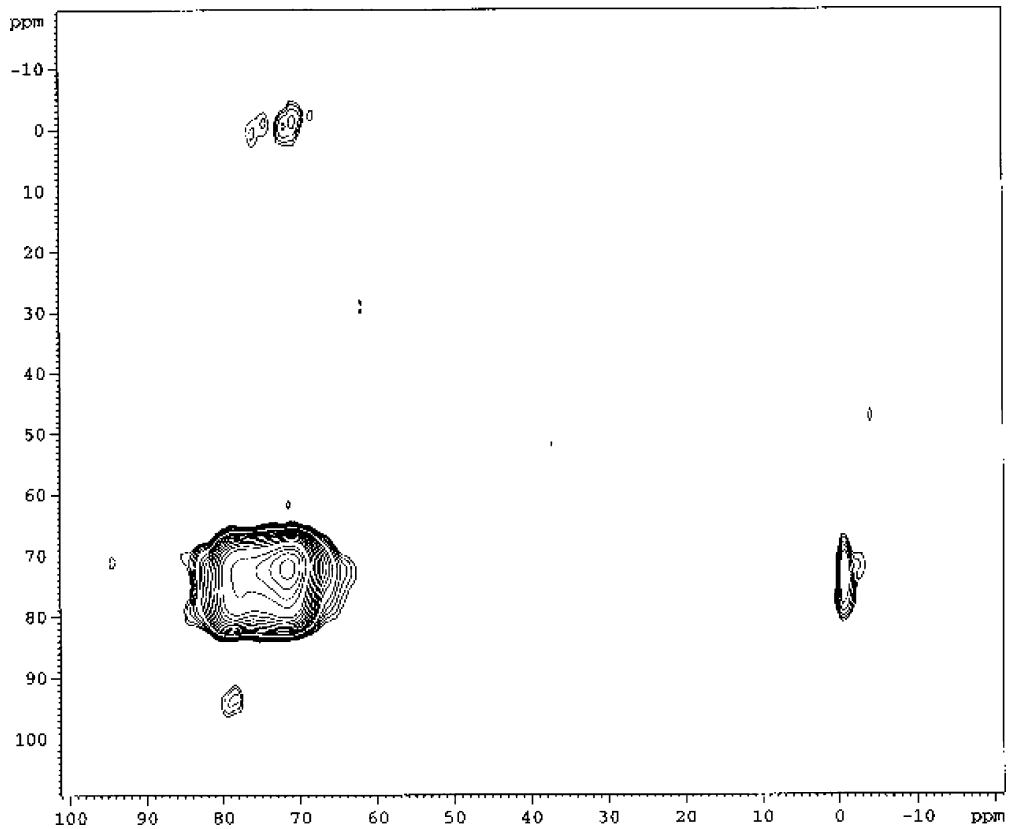

Figure 8. ^{129}Xe 2D EXSY NMR spectrum of IRMOF-2 at room temperature with 32 scans, 80 s repeat time, TD1 of 64, and a mix time of 500 ms.

spectrum taken at the same temperature (Figure 6b), the intensity of the CP spectrum is much lower and the chemical shift is higher. The lower intensity of the CP spectrum is an indication that only a small portion of the adsorbed Xe is in close proximity to the ^{1}Hs. At higher temperatures, no CP signal was observed for ^{129}Xe. It is possible that at higher temperatures xenon molecules are too far removed from the ^{1}H nuclei or too dynamic for successful cross-polarization. The xenon either adsorbs in a location that is not adjacent to the ring (carboxylate groups or tetrahedral Zn_4O corners) or is very weakly adsorbed, as indicated by the measured enthalpies of adsorption from this study; it also has a residence time too short for successful cross-polarization.

The other three IRMOF samples were similar in that no signal was observed at room temperature, indicating unfavorable conditions for cross-polarization. IRMOF-3 also gave a single peak at −50 °C with a chemical shift of 72 ppm (not shown). In the case of IRMOF-1, the temperature had to be lowered to −90 °C before any signal could be observed. Unlike the HP ^{129}Xe spectrum under flow conditions, which had a shoulder on the downfield side of the main signal, the CP spectrum showed a single symmetrical peak at 66 ppm. It was not possible to cross-polarize ^{129}Xe in IRMOF-2 between room temperature and −100 °C. This would seem to indicate that the xenon nuclei within IRMOF-2 were either too dynamic or too far away from the ^{1}H spins for successful CP to occur. None of the spectra showed a signal for free xenon gas indicating that the exchange of adsorbed xenon into the free gas space occurs slower than the time scale of the CP experiment.

EXSY experiments were performed on the sealed samples at room temperature and under flow conditions down to −100 °C. The combination of longer relaxation times and the need for substantial signal averaging often led to unreasonably long acquisition times for the sealed samples. Under flow conditions, the experiment times are much shorter; however, the recorded spectrum is not under equilibrium conditions and as such is not quantitatively precise. In ^{129}Xe 2D EXSY experiments, exchange between sites with different chemical shifts manifests itself by the appearance of off-diagonal cross-peaks between the signals from the sites in exchange. The intensities of the cross-peaks are proportional to the exchange time (τ) set in the experimental pulse sequence. For the sites without exchange (or when the exchange time τ is set very short), only intensity on the main diagonal will appear in the spectrum.

The 2D EXSY spectra of IRMOF-2 under HP xenon flow conditions at temperatures ranging from 35 to −100 °C (Figure 7) displayed exchange between the xenon adsorption sites on a time scale of tens of milliseconds. On the basis of the minimum τ necessary for the appearance of off-diagonal peaks, exchange between the adsorption sites and free gas is less than 50 ms at room temperature. At temperatures below −30 °C, exchange between the free gas and the smaller cavity adsorption site takes longer than 50 ms. This is noted from the lack of cross-peaks between the free gas and adsorption site at higher chemical shift. Exchange between the adsorption sites continues to occur in less than 50 ms at temperatures down to −100 °C. The free gas peak is not observed in the EXSY spectra at −100 °C as it has a very low intensity at this temperature.

The 2D EXSY spectra of the sealed IRMOF samples reveal that exchange between the adsorption sites of xenon also occur on a time scale of tens of milliseconds. In the case of IRMOF-2, it takes $\tau = 15$ ms for exchange between the xenon atoms in the two adsorbed environments to be observed. For exchange to occur between the free gas and adsorbed sites, it was found to take about 500 ms (Figure 8). Such a protracted exchange time may appear to be excessively long but could in fact result from the relatively large path length through the IRMOF

crystallites. A similar rate of exchange was also observed for IRMOF-1 (not shown).

Conclusions

Xenon gas was found to show an affinity for the IRMOF materials and behaved as an efficient probe molecule revealing a variety of different adsorption sites. The heats of xenon adsorption extracted from variable-temperature HP ^{129}Xe NMR were found to be considerably smaller than would be expected for physisorbed xenon. This was attributed to the presence of few binding sites within the very open frameworks of the IRMOF materials. The low heats of adsorption were confirmed by adsorption isotherm measurements that found two xenon atoms per cage under one atmosphere of pressure and a temperature of 19 °C. On the basis of ^{129}Xe NMR data, the pore sizes of the large cavities in the IRMOF networks were estimated and compared with the diameters reported from single-crystal X-ray diffraction experiments. The exchange of xenon from adsorption sites within the IRMOF to the free gas space took about 500 ms while exchange observed between adsorption sites required about 15 ms. From the cross-polarization experiments, which would only be successful at short Xe−H internuclear distances, it was shown that the preferred adsorption sites must be spatially removed from the phenylene rings of the network. This was found to agree well with previously reported gas adsorption studies that showed preferred binding sites for localization of H_2 and Ar near the carboxylate groups and the oxygen-centered tetrahedral Zn_4O corners.

References and Notes

(1) Eddaoudi, M.; Kim, J.; Rosi, N.; Vodak, D.; Wachter, J.; O'Keeffe, M.; Yaghi, O. M. *Science* **2002**, *295*, 469.

(2) Li, H.; Eddaoudi, M.; O'Keeffe, M.; Yaghi, O. M. *Nature* **1999**, *402*, 276.

(3) Chen, B.; Ockwig, N. W.; Millward, A. R.; Contreras, D. S.; Yaghi, O. M. *Angew. Chem., Int. Ed.* **2005**, *44*, 4745.

(4) Rowsell, J. L. C.; Yaghi, O. M. *Angew. Chem., Int. Ed.* **2005**, *44*, 4670.

(5) Rosi, N. L.; Eckert, J.; Eddaoudi, M.; Vodak, D. T.; Kim, J.; O'Keeffe, M.; Yaghi, O. M. *Science* **2003**, *300*, 1127.

(6) Rowsell, J. L. C.; Eckert, J.; Yaghi, O. M. *J. Am. Chem. Soc.* **2005**, *127*, 14904.

(7) Bordiga, S.; Vitillo, J. G.; Ricchiardi, G.; Regli, L.; Cocina, D.; Zecchina, A.; Arstad, B.; Bjorgen, M.; Hafizovic, J.; Lillerud, K. P. *J. Phys. Chem. B* **2005**, *109*, 18237.

(8) Moudrakovski, I. L.; Ratcliffe, C. I.; Ripmeester, J. A. *Appl. Magn. Reson.* **1996**, *10*, 559.

(9) Jameson, C. J.; Jameson, A. K.; Gerald, R. E., II; Lim, H.-M. *J. Phys. Chem. B* **1997**, *101*, 8418.

(10) Chen, Q. J.; Springuel-Huet, M. A.; Fraissard, J. *Chem Phys. Lett.* **1989**, *159*, 117.

(11) Ripmeester, J. A.; Ratcliffe, C. I. *J. Phys. Chem.* **1995**, *99*, 619.

(12) Moudrakovski, I. L.; Ratcliffe, C. I.; Ripmeester, J. A. In *Zeolites: A Refined Tool for Designing Catalytic Sites*; Bonneviot, L., Kaliaguine, S., Eds.; Elsevier Science: New York, 1995.

(13) Morgan, D. R.; Stejskal, E. O.; Andrady, A. L. *Macromolecules*, **1999**, *32*, 1897.

(14) Suzuki, T.; Miyauchi, M.; Yoshimizu, H.; Tsujita, Y. *Polym. J.* **2001**, *33*, 934.

(15) Wang, Y.; Inglefield, P. T.; Jones, A. A. *J. Polym. Sci. B* **2002**, *40*, 1965.

(16) Golemme, G.; Nagy, J. B.; Fonseca, A.; Algieri, C.; Yampolskii, Y. *Polymer* **2003**, *44*, 5039.

(17) Sozzani, P.; Comotti, A.; Simonutti, R.; Meersmann, T.; Logan, J. W.; Pines, A. *Angew. Chem., Int. Ed.* **2000**, *39*, 2695.

(18) Ripmeester, J. A. *J. Am. Chem. Soc.* **1982**, *104*, 289.

(19) Ito, T.; Fraissard, J. *J. Chem. Phys.* **1982**, *76*, 5225.

(20) Ratcliffe, C. I. *Annu. Rep. NMR Spectrosc.* **1998**, *36*, 124.

(21) Raftery, D.; Chmelka, B. F. *NMR: Basic Princ. Prog.* **1994**, *30*, 111.

(22) (a) Grover, B. C. *Phys. Rev. Lett.* **1978**, *40*, 391. (b) Happer, W.; Miron, E.; Schaefer, S.; Schreiber, D.; van Wingaarden, W. A.; Zeng, X. *Phys. Rev. A* **1984**, *29*, 3092. (c) Driehuys, B.; Cates, G. D.; Miron, E.; Sauer, K.; Walter, D. K.; Happer, W. *Appl. Phys. Lett.* **1996**, *69*, 1668.

(23) Rowsell, J. L. C.; Yaghi, O. M. *J. Am. Chem. Soc.* **2006**, *128*, 1304.

(24) Moudrakovski, I. L.; Ratcliffe, C. I.; Ripmeester, J. A.; Wang, L.-Q; Exarhos, G. J.; Baumann, T. F.; Satche, J. H. *J. Phys. Chem. B* **2005**, *109*, 11215.

(25) Terskikh, V. V.; Moudrakovski, I. L.; Du, H.; Ratcliffe, C. I.; Ripmeester, J. A. *J. Am. Chem. Soc.* **2001**, *123*, 10399.

(26) Moudrakovski, I. L.; Lang, S.; Ratcliffe, C. I.; Simard, B.; Santyr, G.; Ripmeester, J. A. *J. Magn. Res.* **2000**, *144*, 372.

(27) Driehuys, B.; Cates, G. D.; Miron, E.; Sauer, K.; Walter, D. K.; Happer, W. *Appl. Phys. Lett.* **1996**, *69*, 1668.

(28) Bielecki, A. A.; Burum, D. *J. Magn. Res*. **1995**, *116*, 215.

(29) Larsen, R. G.; Shore, J. S.; Schmidt-Rohr, K.; Emsley, L.; Long, H.; Pines, A.; Janicke, M.; Chmelka, B. F. *Chem. Phys. Lett.* **1993**, *214*, 220.

(30) Kritzenberger, J.; Gaede, H. C.; Shore, J.; Pines, A. *J. Phys. Chem.* **1994**, *98*, 10173.

(31) Moudrakovski, I. L.; Ratcliffe, C. I.; Ripmeester, J. A. *J. Am. Chem. Soc.* **1998**, *120*, 3123.

(32) Moudrakovski, I. L.; Ratcliffe, C. I.; Ripmeester, J. A. *Appl. Magn. Reson.* **1995**, *8*, 385.

(33) Zhu, X.; Moudrakovski, I. L.; Ripmeester, J. A. *Energy Fuels* **1997**, *11*, 245.

(34) Kentgens, A. P. M.; Van Boxtel, H. A.; Verweel, R. J.; Veeman, W. S. *Macromolecules* **1991**, *24*, 3712.

(35) Rowsell, J. L. C.; Spencer, E. C.; Eckert, J.; Howard, J. A. K.; Yaghi, O. M. *Science* **2005**, *309*, 1350.

(36) Yildirim, T.; Hartman, M. R. *Phys. Rev. Lett.* **2005**, *95*, 215504.

(37) Spencer, E. C.; Howard, J. A. K.; McIntyre, G. J.; Rowsell, J. L. C.; Yaghi, O. M. *Chem. Commun.* **2006**, 278.

(38) Sagara, T.; Klassen, J.; Ganz, E. *J. Chem. Phys.* **2004**, *121*, 12543.

(39) Sagara, T.; Klassen, J.; Ortony, J.; Ganz, E. *J. Chem. Phys.* **2005**, *123*, 014701.

(40) Sarkisov, L.; Düren, T.; Snurr, R. Q. *Mol. Phys.* **2004**, *102*, 211.

(41) Düren, T.; Sarkisov, L.; Yaghi, O. M.; Snurr, R. Q. *Langmuir* **2004**, *20*, 2683.

(42) Mueller, T.; Ceder, G. *J. Phys. Chem. B* **2005**, *109*, 17974.

(43) Mulder, F. M.; Dingemans, T. J.; Wagemaker, M.; Kearley, G. *J. Chem. Phys.* **2005**, *317*, 113.

(44) Terskikh, V. V.; Moudrakovski, I. L.; Mastikhin, V. M. *J. Chem. Soc., Faraday Trans.* **1993**, *89*, 4239.

(45) Moudrakovski, I. L.; Wang, L.-Q.; Baumann, T.; Satcher, J. H., Jr.; Exarhos, G. J.; Ratcliffe, C. I.; Ripmeester, J. A. *J. Am. Chem. Soc*. **2004**, *126*, 5052.

(46) Moudrakovski, I. L.; Terskikh, V. V.; Ratcliffe, C. I.; Ripmeester, J. A.; Wang, L.-Q.; Shin, Y.; Exarhos, G. J. *J. Phys. Chem. B* **2002**, *106*, 5938.

(47) Terskikh, V. V.; Moudrakovski, I. L.; Breeze, S. R.; Lang, S.; Ratcliffe, C. I.; Ripmeester, J. A.; Sayari, A. *Langmuir* **2002**, *18*, 5653.

(48) Huang, S.-J.; Huang, C.-H.; Chen, W.-H.; Sun, X.; Zeng, X.; Lee, H.-K.; Ripmeester, J. A.; Mou, C.-H.; Liu, S.-B. *J. Phys. Chem. B* **2005**, *109*, 681.

(49) Ripmeester, J. A.; Ratcliffe, C. I. *J. Phys. Chem.* **1990**, *94*, 7652.

(50) Soldatov, D. V.; Moudrakovski, I. L.; Grachev, E. V.; Ripmeester, J. A. *J. Am. Chem. Soc*. **2006**, *128* (20), 6737.

(51) Nossov, A. V.; Soldatov, D. V.; Ripmeester, J. A. *J. Am. Chem. Soc.* **2001**, *123*, 3563.

(52) Pines, A.; Gibby, J. S.; Waugh, J. *J. Chem. Phys.* **1972**, *56*, 1756.

(53) Chagolla, D.; Geezman, E.; Ba, Y. *Microporous Mesoporous Mater.* **2003**, *64*, 155.

(54) Jeener, J.; Meier, B. H.; Bachmann, P.; Ernst, R. R. *J. Chem. Phys.* **1979**, *71*, 4546.

(55) Kentgens, A. P. M.; van Boxtel, H. A.; Verweel, R.-J.; Veeman, W. S. *Macromolecules* **1991**, *24*, 3712.

(56) Kritzenberger, J.; Gaede, H. C.; Shore, J. S.; Pines, A.; Bell, A. T. *J. Phys. Chem.* **1994**, *98*, 10173.

(57) Larsen, R. G.; Shore, J.; Schmidt-Rohr, K.; Emsley, L.; Pines, A.; Janicke, M.; Chmelka, B. F. *Chem. Phys. Lett.* **1993**, *214*, 220.

(58) Kolodziejski, W.; Klinowski, J. *Chem. Rev*. **2002**, *102*, 613.